Multi-stage pseudomorphic replacement of garnet during polymetamorphism: 1. Microstructures and their interpretation

B. CESARE
CNR Centro di Studio per la Geodinamica Alpina, and Dipartimento di Mineralogia e Petrologia – Università di Padova, Corso Garibaldi 37, I-35137 Padova, Italy (bernardo@dmp.unipd.it)

ABSTRACT

Metapelites from the southern aureole of the Vedrette di Ries tonalite (eastern Alps) were variably overprinted by contact and earlier regional metamorphic events during pre-Alpine and Alpine metamorphic cycles. In these rocks, starting from a primary garnet mica-schist (garnet stage), a complex sequence of transformations, affecting the site of the garnet, has been recognized. In the outermost part of the aureole, the primary garnet sites are occupied by nodules of kyanite (kyanite stage). Closer to the tonalite, kyanite is replaced by staurolite (staurolite stage), which in turn is pseudomorphed by muscovite (muscovite stage). The aggregates of kyanite do not overgrow garnet directly; they post-date a stage (fibrolite stage) represented by the pseudomorphic alteration of garnet into fibrolitic sillimanite plus biotite. A further sericite stage is likely to have occurred between the fibrolite and kyanite stages. Preservation of the sub-spherical garnet shape during all these transformations and persistence of mineralogical and textural relicts from earlier stages were favoured by the very low strain experienced by the rocks since the garnet stage. The textural sequence is in agreement with the metamorphic history of this part of the Austroalpine basement of the Eastern Alps: the garnet and fibrolite stages, and the coeval main foliation of the samples, are referred to the high-grade Hercynian metamorphism; the kyanite stage to the Eo-Alpine metamorphism; the staurolite and muscovite stages to the Oligocene contact metamorphism. It is suggested that kyanite growth as microgranular aggregates took place in polymetamorphic rocks where static, high-P/low-T metamorphism overprinted high-T assemblages that contained sillimanite or andalusite.

Key words: garnet; microgranular kyanite; microstructure; polymetamorphism; pseudomorph.

INTRODUCTION

Recognition and characterization of superimposed metamorphic episodes, either during a continuous polyphase P–T path (e.g. subduction–collision–exhumation, Selverstone, 1985) or during repeated cycles of polymetamorphism (e.g. 'Caledonian'–Hercynian–Alpine evolution of the Eastern Alps) are critical for the understanding of the tectonic evolution of a metamorphic basement. This is commonly achieved through the study of metastable minerals within the main paragenesis, based on microstructural analysis and/or chemical compatibility. The occurrence of metastable relicts reflects incomplete re-equilibration at the new metamorphic conditions, which depends on: (i) the temperature and duration of metamorphism (e.g. Ridley, 1985); (ii) the availability of fluids during retrograde, hydration processes (e.g. Fyfe *et al.*, 1978); and (iii) the intensity of deformation. Deformation is particularly important in the process of re-equilibration, because it accelerates reaction progress and allows fluid circulation and redistribution within the rock (e.g. Brodie & Rutter, 1985). Thus, metastable persistence of relict minerals is favoured when one or more of the following conditions are attained: (i) lower-grade metamorphism overprints higher-grade; (ii) metamorphism occurs without, or with very low, concomitant strain; (iii) the duration of the metamorphic overprint is short, such as during contact metamorphism.

Owing to the presence of all the above favourable conditions, some pelitic schists in the aureole of Vedrette di Ries have preserved a long microstructural memory, enclosed within peculiar nodular textures and in the adjacent matrix. This paper describes and discusses the microstructures of these rocks, with particular emphasis on the complex sequence of pseudomorphs involving a primary garnet. The interpretation of microstructures is then used to refine the geological and metamorphic evolution of this area, and to propose a model for the origin of microgranular kyanite.

GEOLOGICAL SETTING

In the region between the Tauern Window and the Periadriatic Lineament (PL), the Austroalpine basement of the Eastern Aps forms an E–W-trending belt, divided into three blocks by two major tectonic lines: the Deferegger–Anterselva–Valles (DAV) line and the Kalkstein–Vallarga (KV) line (Fig. 1a).

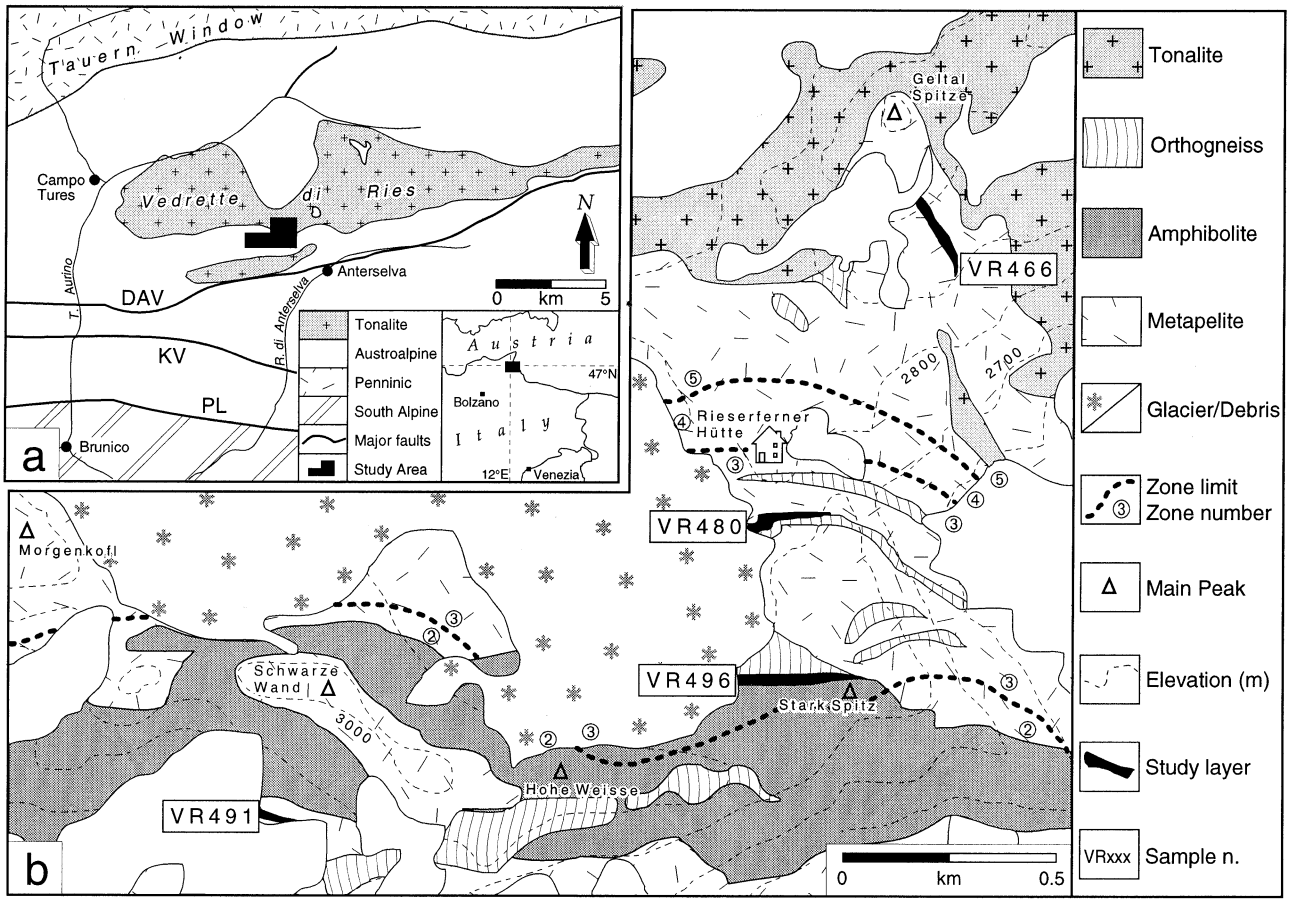

Fig. 1. (a) Tectonic sketch map of the region of Vedrette di Ries. (b) Simplified geological map (after Mager, 1985) of the southern aureole of Vedrette di Ries, with location of the study rock layers and respective sample numbers. Mineral zones as in Table 1.

Unlike the other two blocks, which display an essentially pre-Alpine tectono-metamorphic history, the block north of the DAV line was involved in the Alpine metamorphic cycle (Borsi *et al.*, 1978): its polymetamorphic history is complex, and, to some extent, still controversial, and can be summarized as follows:

1 'Caledonian' metamorphism of undetermined P–T conditions (Borsi *et al.*, 1973);

2 Hercynian high-grade metamorphism and anatexis at $P = 6 \pm 1$ kbar and $T = 650$ °C (Stöckhert, 1985, 1987);

3 Eo-Alpine metamorphism under relatively high-P/low-T conditions (7.5 ± 1.5 kbar and 450 ± 50 °C, Stöckhert, 1987);

4 'Main Alpine' ('*Tauern*') metamorphism under lower greenschist facies conditions (Sassi *et al.*, 1980);

5 Oligocene contact metamorphism in the aureole of the Vedrette di Ries pluton (Cesare, 1994): the last metamorphic event recorded in the area.

The main Alpine metamorphism was accompanied by intense deformation that produced a widespread mylonitic schistosity in the metapelites (Kleinschrodt, 1987). However, parts of the block escaped the Alpine structural reworking (not the metamorphic overprint) and still preserve pre-Alpine structures and metamorphic relict assemblages (Borsi *et al.*, 1978). One such area is located south of the Vedrette di Ries pluton, which has dominant metapelites, with minor interbedded layers of pegmatite gneiss, marble, quartzite and amphibolite (Mager, 1985). The metamorphic layering is isoclinally folded, strikes E–W and dips south at 30–60°.

The southern contact aureole of the Vedrette di Ries tonalite is *c.* 1.5 km in thickness and has six mineralogical zones (Table 1) that developed at $P = 2.5$–3.75 kbar and peak $T = 600$–620 °C (Cesare, 1994). A weak deformation, occurring as a reactivation of the earlier

Table 1. Mineral zones of contact metamorphism in the southern aureole of Vedrette di Ries.

Zone	Name	AFM assemblage
1	chlorite–biotite	Bt–Chl–Grt (+Ms+Qtz)
2	biotite–staurolite	Bt–Chl–St (+Ms+Qtz)
3	staurolite–andalusite	Bt–Chl–St–And (+Ms+Qtz)
4	staurolite–fibrolite	Bt–St–Fib (+Ms+Qtz)
5	fibrolite–garnet	Bt–Grt–Fib (+Ms+Qtz)
6	'second sillimanite'	Bt–Grt–Sil (+Kfs+Qtz)

main foliation, accompanied contact metamorphism and is localized in the zones of highest metamorphic grade, close to the pluton contact.

Within the metapelites, layers of a distinctive rock type crop out in at least four localities at variable distance from the intrusive contact (Fig. 1b). The layers have a thickness of <20 m, and consist of fine-grained mica-schists with a marked millimetric compositional layering, with abundant quartz-rich ribbons, probably the result of mylonitic deformation. The foliation wraps around lensoid domains in which garnet, kyanite, staurolite, andalusite or muscovite are in turn dominant. The systematic distribution of Al_2SiO_5 polymorphs in the aureole and the resulting isograd pattern (Fig. 1 & Table 1) indicate that during the contact metamorphic event only the layer closest to the contact (i.e. sample VR466) reached temperatures sufficient for the crystallization of sillimanite. It follows that in all the other layers any occurrence of sillimanite is attributable to earlier metamorphism. Both field appearance and microstructural characteristics suggest that these rocks, although showing different mineralogy at each locality, may represent the same primary rock type (the same folded layer?), variably transformed during the complex metamorphic evolution of this area. Study of these rocks provides the opportunity to distinguish between the succession of five metamorphic events that are postulated to have affected the area. In fact, previous microstructural works on the metapelites of this part of the Austroalpine basement have mainly focussed either on the pre-Alpine (e.g. Sassi *et al.*, 1987) or the Alpine (e.g. Contini & Sassi, 1980), or the contact metamorphic history (e.g. Cesare, 1994). These studies have sometimes led to conflicting interpretations, as for the age of the aggregates of microgranular kyanite, which have been ascribed both to the Hercynian (e.g. Mazzoli & Moretti, 1998) and to the Eo-Alpine metamorphism (e.g. Bellieni, 1974).

SAMPLE DESCRIPTION

Four representative samples have been chosen, one at each locality in Fig. 1(b), and used for microstructural study, bulk chemical, and mineral chemical analysis.

VR491 (zone 2 (biotite–staurolite) of contact metamorphism) is the furthest from the intrusive contact. It is a muscovite-rich schist, with a well-developed, millimetre-spaced schistosity, axial plane to a relict crenulation preserved in the microlithons. The rock contains nodular segregations (hereafter referred as '*nodules*') of kyanite, typically <5 mm in diameter; garnet occurs as isolated porphyroblasts, or associated with kyanite in the aggregates.

VR496 (outer zone 3 (andalusite–staurolite)) is a strongly layered but massive mica-schist, rich in garnet porphyroblasts and nodules of fine-grained, brown staurolite. Andalusite crystals, up to 3 cm in length, occur in the muscovite-rich layers of the matrix.

VR480 (inner zone 3) is a mica-schist with nodules of microgranular staurolite up to 1 cm in diameter. Large porphyroblasts of andalusite occur in the mica-rich layers, which also contain biotite, muscovite and staurolite. Quartz layers may reach one cm in thickness.

VR466 (zone 5 (fibrolite–garnet)) is a biotite-rich schist some 50 m distant from the contact. Biotite layers alternate with quartz ribbons and fibrolite-rich folia ('fibrolite' refers to the fine-grained, acicular variety of sillimanite). Pink andalusite porphyroblasts are abundant, whereas the scarce muscovite is mainly concentrated in millimetre-sized nodules.

Fig. 2 shows the textures of the four samples, which have nodules (enlarged in Fig. 2e–h) of comparable size and distribution in the matrix. In addition, all rocks have similar quartz-rich ribbons, are graphitic, and contain tourmaline with similar, complex zoning. In the transition from sample VR491 to sample VR466, there is a progressive coarsening of matrix minerals (quartz, biotite and muscovite), minerals within nodules (e.g. staurolite) and the nodules themselves. This is consistent with the increasing temperature and duration of contact metamorphism in the samples approaching the pluton.

MICROSTRUCTURAL ANALYSIS

The microstructural analysis is focused on the evolution of nodules, and on the assessment of the related possible reactions and reaction mechanisms. In the following section, fine-grained ('sericite') and coarse-grained muscovite are distinguished because they have different chemical composition (see below) and generally occur in different microstructural sites: sericite in felts associated with the nodules; muscovite in the micaceous layers that define the foliation. For each sample, *nodules* and adjacent *matrix* are described separately.

Sample VR491

The nodules are sub-spherical aggregates of randomly oriented, microgranular (100–200 μm) kyanite with minor biotite, quartz and ilmenite (Fig. 2e). Garnet is commonly associated with the kyanite aggregates, either as relicts within the nodules, or more rarely as porphyroblasts with a thin, discontinuous corona of kyanite (Fig. 3a). In the latter texture, the size of garnet porphyroblast is comparable to that of the adjacent kyanite nodule. Staurolite is also present in the nodules as rare fine-grained crystals rimming kyanite. Most nodules of kyanite are enclosed in a fine-grained felt of sericite, and where a kyanite crystal abuts sericite it is euhedral. Fibrolite also occurs in the outer parts of the nodules as inclusions within quartz (Fig. 3b) or coarse-grained muscovite that are separated from the kyanite aggregates by a thin layer of sericite. Fibrolite shows euhedral terminations within the host crystals, but is truncated and replaced at the host-sericite grain boundary (Fig. 3c). It never occurs in the sericite matrix, in contact with kyanite, or in the micaceous layers surrounding the nodules.

The matrix is composed of alternating quartz-rich and muscovite–biotite layers, mainly oriented parallel to the foliation, or tracing relict folds within microlithons. A further textural generation of biotite, muscovite and chlorite is recognized in the finer-grained lamellae that statically overgrow the foliation or crystallize in the sericite felts. Garnet, ilmenite, sericite and kyanite also occur in the micaceous layers. Garnet

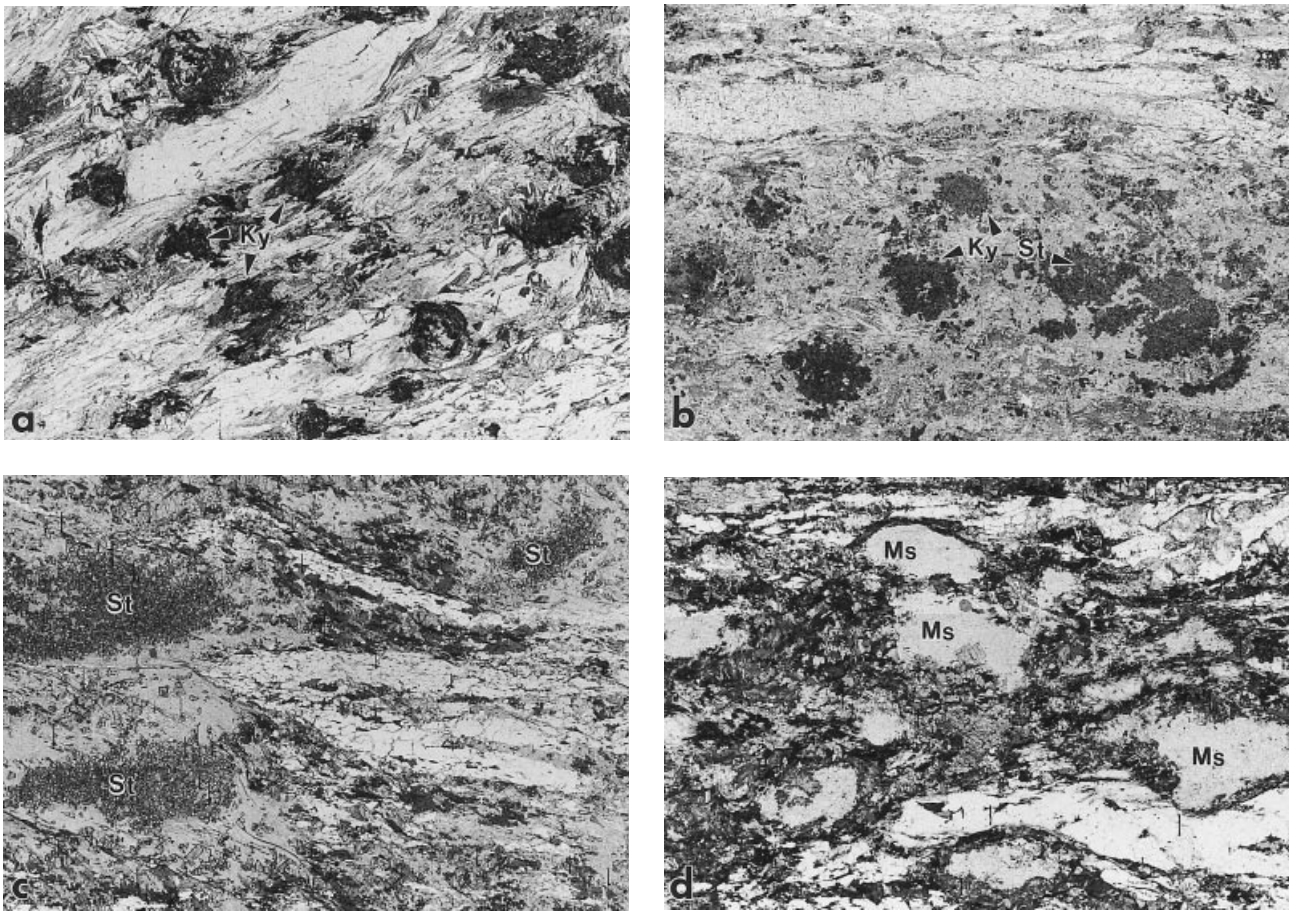

Fig. 2. (a)–(d) Photomicrographs illustrating the main textural relationships among nodules, matrix and main foliation in the study samples. Plane-polarized light (PL), width of view (wv) = 40 mm. (a) VR491 with Ky-rich nodules; (b) VR496 with Ky + St nodules; (c) VR480 with St-rich nodules; (d) VR466 with Ms-rich nodules. (e)–(h) Close-up views of nodules from each sample. (e) VR491. Round aggregate of microgranular kyanite with minor biotite, ilmenite and garnet. Two kyanite-rich asymmetric tails (arrows) extend in the sub-horizontal main foliation. PL, wv = 6.5 mm. (f) VR496. Nodule of kyanite and staurolite. Kyanite occurs at the core of most staurolite crystals (asterisks). Crossed polars (CP), wv = 6.5 mm. (g) VR480. Monomineralic nodule of staurolite in a sericite felt (ser). Note (arrows) the coarser grain size of staurolite in the periphery of the aggregate, or isolated in the sericite matrix. Sericite around nodule (lower right) shows preferred orientation with incipient shear band cleavage. This suggests reactivation of the main foliation during contact metamorphism. PL, wv = 6.5 mm. (h) VR466. Decussate monomineralic aggregate of muscovite wrapped by folia of biotite and fibrolite. PL, wv = 6.5 mm.

is small and euhedral, rich in ilmenite inclusions, and overgrows biotite. Kyanite is also very fine-grained, and always associated with sericite, but in the matrix, it does not replace fine-grained garnet. Plagioclase occurs both in micaceous and quartz-rich layers.

Sample VR496

Sample VR496 shows several affinities to VR491: (a) fibrolite forms rare inclusions in quartz; (b) the nodules are enclosed in a sericitic felt; (c) garnet in the nodules as well as in the matrix has the same microstructural features of sample VR491. The nodules consist of microgranular staurolite and kyanite (Fig. 2f), with minor ilmenite and garnet relicts. Staurolite may form thin coronas around garnet porphyroblasts (Fig. 4a), and forms by epitaxial replacement of kyanite, where it has homogeneous rims and oriented kyanite in the core (Fig. 4b, see also Cesare & Grobety, 1995). Staurolite in the outer nodule, in contact with the sericite-rich matrix, is euhedral and coarser than in the nodule core. The sericite-rich matrix adjacent to the nodules contains euhedral, randomly oriented crystals of chlorite and biotite, but biotite does not occur within the nodules. Andalusite porphyroblasts overgrow the main foliation and are preferentially located in the sericite-rich matrix adjacent to the nodules, where they may enclose part of the nodules, as well as flakes of biotite. The inclusions of biotite and staurolite in andalusite are smaller, compared with the average grain size of the same minerals outside andalusite (Fig. 4c), implying that andalusite and staurolite growth, and the coarsening of the matrix were, at least in part, synchronous.

In the micaceous matrix, biotite and chlorite are randomly oriented, and the amount of muscovite

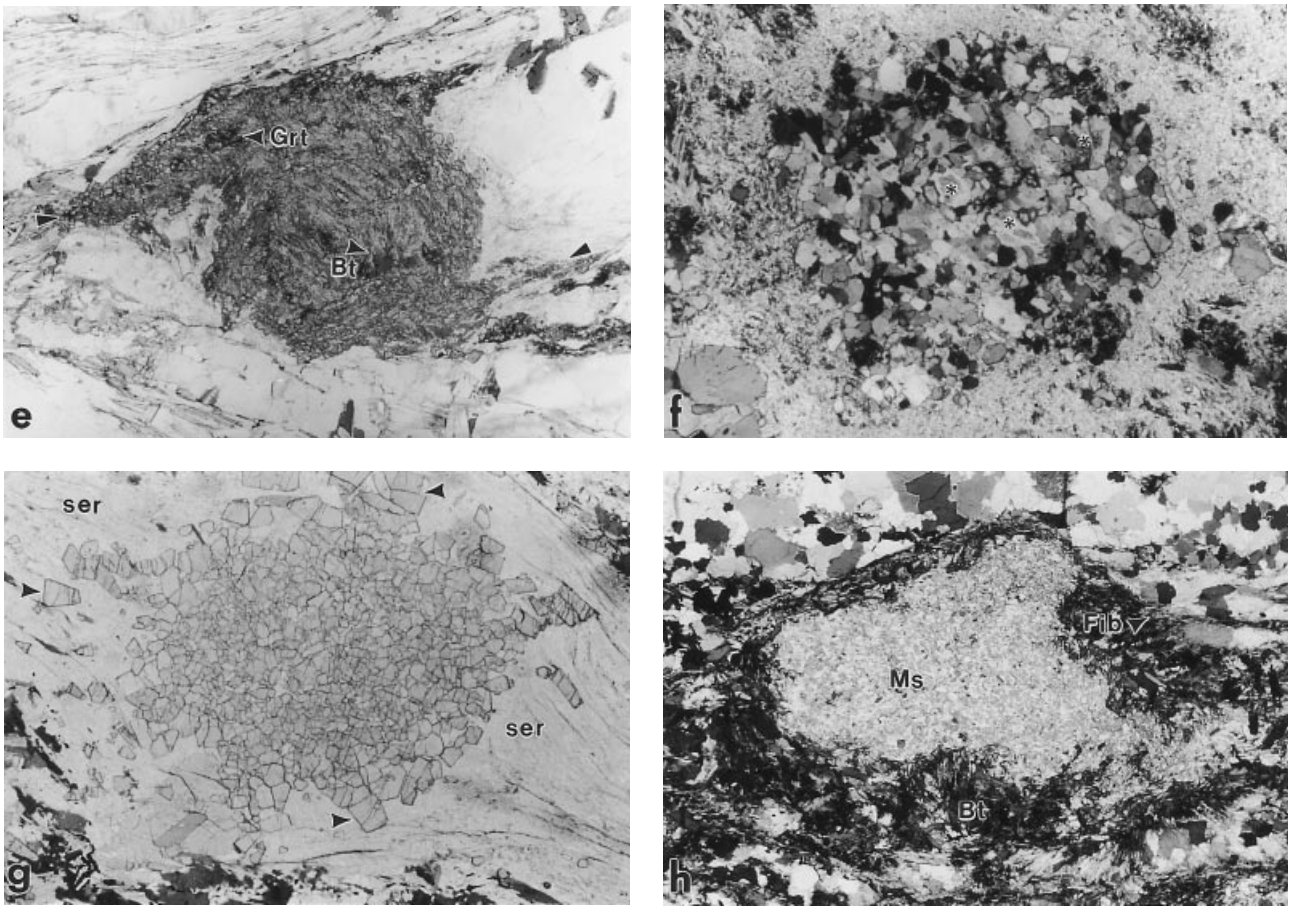

Fig. 2. (*Continued*)

decreases. As in sample VR491, fine-grained garnet rimming biotite is rather common. Isolated crystals of staurolite statically overgrow the foliation, as indicated by straight inclusion trails continuing without deflection in the external foliation. The amount of plagioclase is again quite low.

Sample VR480

These nodules contain only microgranular staurolite (Fig. 2g) that has no kyanite inclusions. Similarly, garnet relicts or ilmenite, common within the nodules of the previous samples, have not been observed. Sericite is abundant in the felts surrounding the nodules, and is coarser than in sample VR496. In these domains, a local preferred orientation of sericite defines incipient shear bands inferred to represent reactivation of the main foliation during contact metamorphism (Fig. 2g).

In the matrix, biotite and staurolite are very abundant, chlorite, plagioclase and muscovite are scarce, and kyanite is absent. Chlorite is in textural equilibrium with staurolite, andalusite and biotite. The fine-grained garnet, commonly associated with biotite in the previous samples, occurs only as rare armoured relicts within biotite, staurolite or andalusite.

Sample VR466

The nodules are almost monomineralic, decussate aggregates of muscovite (Fig. 2h). In places, muscovite contains inclusions of staurolite a few tens of microns in size (Fig. 5a), with rounded borders and random orientation. These inclusions are armoured within single muscovite crystals, and never cut grain boundaries. Relicts of staurolite also occur, together with biotite, within centimetre-sized porphyroblasts of andalusite. Staurolite inclusions in andalusite are randomly orientated, are similar in size to those in muscovite, but are commonly euhedral.

Muscovite nodules and andalusite porphyroblasts are surrounded by biotite-rich layers that form most of the rock matrix. Unlike samples VR491 and VR496, fibrolite is abundant in the biotite layers, and forms either thin folia with strong preferred orientation parallel to the foliation, or sheaves radiating from biotite grains. Because this generation of fibrolite has grown after the final positioning of grain boundaries

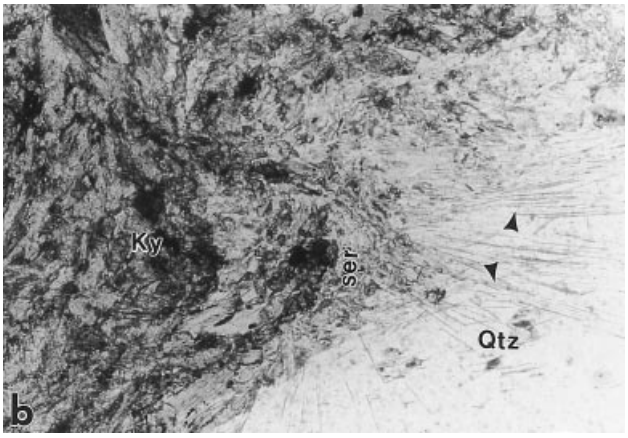

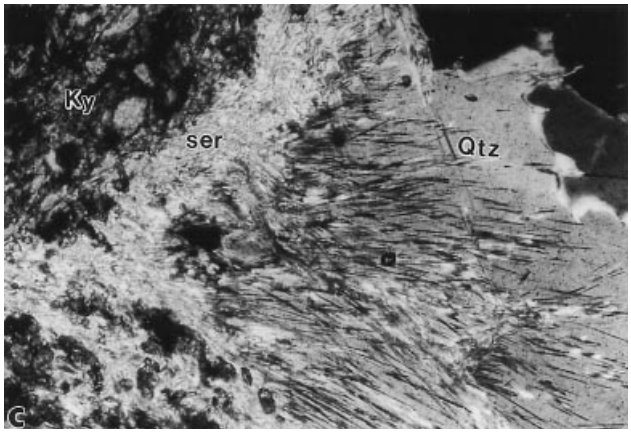

Fig. 3. (a) VR491. Ky-rich nodule adjacent to an almost euhedral crystal of garnet with thin, discontinuous rim of kyanite (arrows). The size of garnet is comparable to that of the kyanite nodule. PL, wv = 11 mm. (b) VR491. Textural relationships between kyanite, sericite and fibrolite in the outer part of a Ky-rich nodule. A thin sericite layer is present between the nodule and the adjacent quartz; coarse quartz contains fibrolite needles (arrows) radiating from the nodule. PL, wv = 1.1 mm. (c) VR491. Close-up of the border of a kyanite nodule. Fibrolite is only present within quartz in the right-hand side of the picture, and is truncated at the quartz–sericite interface. It follows that all fibrolite crystals are relict inclusions within quartz. Crossed polars (CP), wv = 0.5 mm.

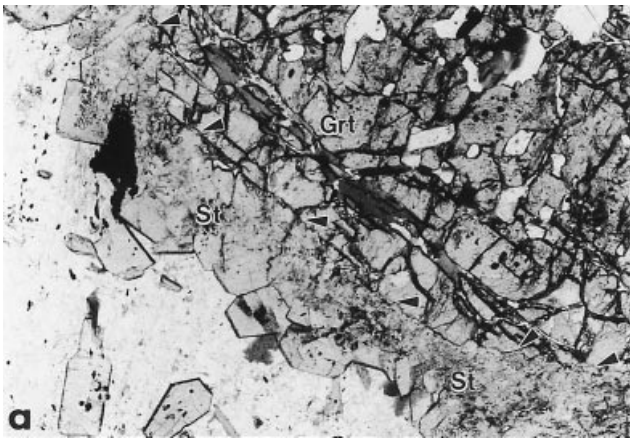

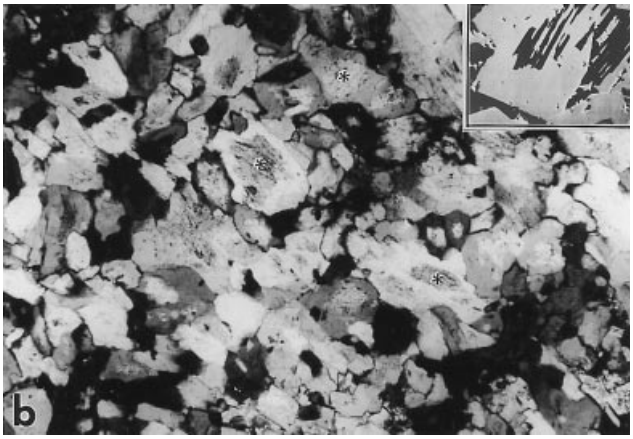

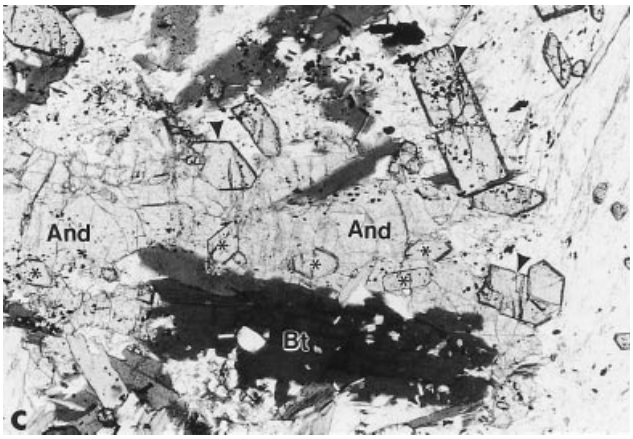

Fig. 4. (a) VR496. Polycrystalline corona of staurolite around a porphyroblast of garnet. Arrows mark garnet grain boundary. PL, wv = 1.1 mm. (b) VR496. Detail of Fig. 2(f), showing the abundance of kyanite (asterisks) at the core of staurolite. PL, wv = 2.2 mm. Inset: back-scattered SEM image of staurolite crystals (bright) with kyanite cores (black). Kyanite forms epitaxially oriented lamellae within staurolite (wv = 120 μm). (c) VR496. Euhedral staurolite inclusions in andalusite (asterisks) are finer than staurolite in the adjacent matrix (arrows). This relationship suggests simultaneous growth of andalusite and staurolite. PL, wv = 1.1 mm.

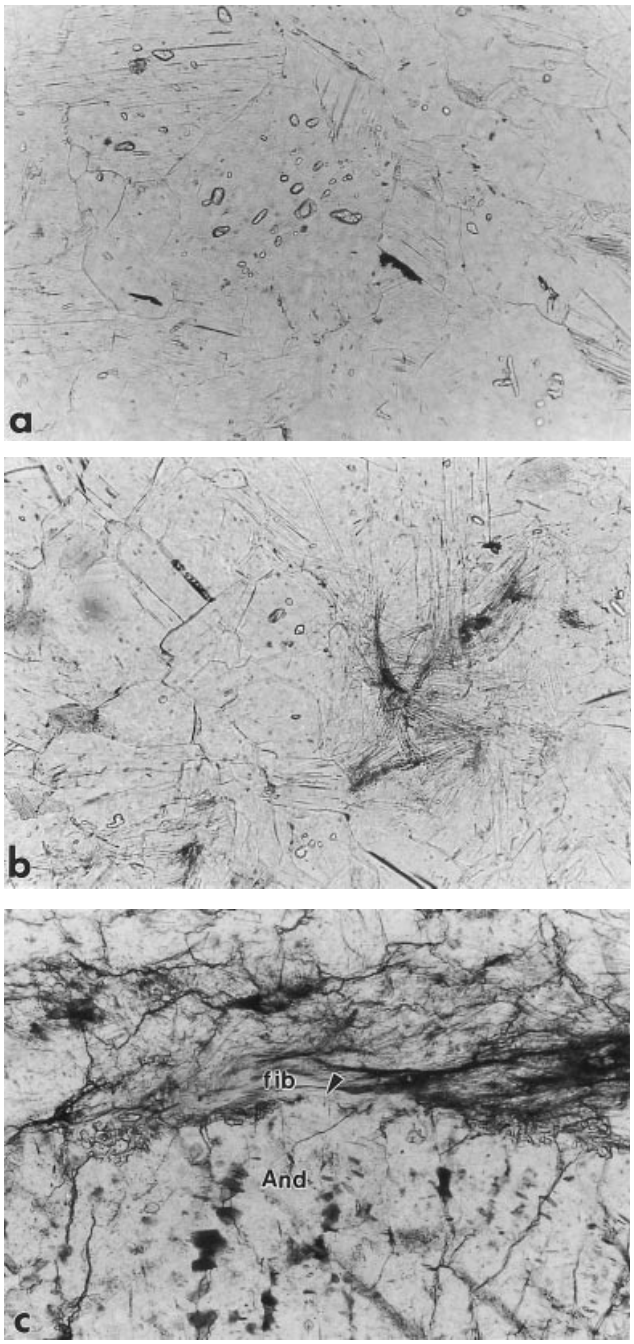

Fig. 5. (a) VR466. Fine-grained staurolite inclusions in muscovite from a nodule in Fig. 2(d) have round shape and do not crosscut muscovite grain boundaries, suggesting resorption. Inclusions have random orientation and cannot derive from a former large porphyroblast. PL, wv = 0.5 mm. (b) VR466. Intergrowth of fibrolite$_2$ and muscovite in a muscovite nodule indicates that growth of fibrolite$_2$ occurs after the final positioning of muscovite grain boudaries. PL, wv = 0.5 mm. (c) VR466. Fibrolite$_2$-rich folia (fib) around andalusite. The rounded grain boundary of andalusite abutting fibrolite (arrow) is an indication for andalusite dissolution and stability of sillimanite. PL, wv = 1.1 mm.

of adjacent matrix minerals, it must be of contact metamorphic origin, and is here defined as fibrolite$_2$. The boundary between muscovite nodules and the biotite–fibrolite$_2$ matrix is sharp, with only minor fibrolite$_2$ intergrown with muscovite (Fig. 5b).

In the matrix, muscovite forms rare resorbed crystals in the biotite layers; chlorite, staurolite and garnet have not been observed. Conversely, plagioclase is more abundant than in the previous samples. Andalusite forms individual, unstrained porphyroblasts, or radiating aggregates with undulose extinction. Along with quartz and biotite, andalusite is locally dissolved in the areas abutting fibrolite$_2$ folia (Fig. 5c).

INTERPRETATION OF MICROSTRUCTURES

Sample VR491

The shape of the kyanite-rich nodules and the enclosed garnet relicts are good evidence that the nodules are pseudomorphs after garnet, but there are at least two difficulties in interpreting them as a direct kyanite replacement The first is that pseudomorphs of microgranular kyanite after garnet have not been reported in the literature, with the exception of Wheeler *et al.* (1995). The second is that fibrolite is also present in close association with the nodules; in this perspective, it is notable that Wheeler *et al.* (1995) observed fibrolite within garnet surrounded by microgranular kyanite. Thus, assessment of the relative timing of growth of kyanite and fibrolite is critical for a correct interpretation of kyanite aggregates.

Fibrolite needles are restricted as inclusions in quartz and muscovite, and are replaced by sericite at the host-sericite grain boundary: they are interpreted as relicts pre-dating sericite growth. Conversely, kyanite is widespread in nodules and matrix, and is idioblastic in the sericite felt: these features suggest that kyanite crystallized after (or together with) sericite and is younger than fibrolite. Thus, the inferred crystallization sequence is fibrolite→sericite→kyanite. Because the relationships between sericite and kyanite are ambiguous, the simultaneous growth of sericite and kyanite in a single event is an alternative possibility. This does not invalidate the evidence for an earlier crystallization of fibrolite. Based on the association of fibrolite radiating from the nodules, and on the additional presence of biotite and ilmenite, I suggest that the earlier stages in the evolution of the nodules are represented by a pseudomorph of fibrolite plus biotite after a primary garnet. This kind of pseudomorph is common in upper amphibolite facies metapelites (Yardley, 1977) and has been observed in the adjacent Austroalpine basement (Schulz, 1995). A retrograde hydration event at the expense of fibrolite is considered responsible for the occurrence of sericite aggregates, and for the preservation of fibrolite only as relict inclusions in quartz and coarse muscovite. Kyanite growth post-dates (or is synchronous with)

this event, and is accompanied by the release of Ti from biotite, with growth of ilmenite.

Because sample VR491 belongs to the external part of the contact aureole, where the recrystallization effects were very weak, it follows that most of the metamorphic and textural history of this rock predates the contact metamorphic event. Among the effects of contact metamorphism are the rare rims of staurolite on kyanite, interpreted as the beginning of the epitaxial replacement described below.

Sample VR496

Staurolite crystallization was controlled by the presence of kyanite: owing to the affinity of its crystal lattice, kyanite was replaced by an epitaxial mechanism producing the very distinctive microstructure of nodules of microgranular staurolite. The incomplete replacement left metastable kyanite relicts armoured by staurolite; the stable Al_2SiO_5 polymorph is andalusite. Transformation of kyanite to staurolite requires addition of Fe and Mg to the reaction site (Cesare & Grobety, 1995): this probably occurred by consumption of biotite and garnet, the amounts of which greatly decrease in the nodules, compared to sample VR491.

Sample VR480

The replacement of kyanite by staurolite proceeded to completion, as indicated by the absence of kyanite relicts. The nodules of staurolite seemingly represent direct pseudomorphs after garnet, but are actually pseudomorphs after kyanite within a primary garnet site. Recrystallization during contact metamorphism is almost complete, and only the fine-grained garnet may be a metastable phase. Muscovite in the micaceous layers shows a marked decrease, whereas the fine-grained sericite is still abundant; as a whole, the amount of muscovite decreases with respect to VR496. Preferred dissolution of coarse white mica is probably related to two factors: (a) the different composition of the two micas that stabilizes the low-Ti ($TiO_2 < 0.3$ wt%) sericite with respect to muscovite (TiO_2 *c.* 0.7 wt%); and (b) a kinetic control on dissolution sites that favours dissolution of muscovite located in the recrystallizing biotite-rich layers.

Sample VR466

The round shape of muscovite nodules, their size, and, more importantly, the presence of staurolite inclusions within muscovite, are strong evidence for a genetic relationship between this sample and the previous. Thus, the nodules result from the replacement of former aggregates of microgranular staurolite by decussate muscovite. Staurolite inclusions are finer than in the nodules of sample VR480. This may be related to a higher heating rate in the inner part of the aureole that limits staurolite coarsening prior to replacement by muscovite. In fact, the absence of staurolite in the matrix indicates that the stability of St + Ms + Qtz was exceeded. The prograde nature of the muscovite pseudomorph after staurolite is demonstrated by the intergrowth of fibrolite$_2$ and muscovite in the nodules (Fig. 5b). This texture is similar to those described by Vernon & Flood (1977), and attributed to simultaneous growth during prograde metamorphic reactions. Along with the dissolution of andalusite (cf. Fig. 5c), this indicates that sillimanite is the stable Al_2SiO_5 polymorph in this rock.

Although the amount of muscovite has decreased with respect to sample VR480, this mineral does not simply show dissolution, but a redistribution among the different microstructural sites of the rock. Most muscovite in the micaceous layers and sericite felts surrounding the nodules dissolved, whereas new growth of decussate muscovite occurred in the former staurolite nodule. This texture is similar to that described by Carmichael (1969) for prograde reactions, and confirms, as suggested by sample VR480, the presence of a kinetic control on dissolution/precipitation mechanisms.

Sample VR466 shows the most apparent, albeit weak, effects of syn-deformational contact metamorphism: these include the radiating textures of andalusite, the preferred orientation of fibrolite$_2$, and the dissolution of matrix abutting high-strain zones (cf. Fig. 5c).

POLYMETAMORPHIC EVOLUTION OF A PRIMARY GARNET SITE

The microstructural information allows reconstruction of the complex textural evolution of a primary garnet site, now represented by the nodules. Preservation of the sub-spherical shape of garnet was favoured by the very low strain experienced by these rocks after garnet crystallization, which resulted in the static growth of minerals in all the subsequent metamorphic events. The textural sequence can be divided into five (or six) stages.

Garnet stage (VR491, VR496)

This is the earliest microstructural stage, with garnet porphyroblasts of < 1 cm diameter wrapped by the micaceous layers. Inclusions in garnet consist of quartz, biotite, ilmenite and muscovite, and provide no information on the metamorphic history of the metapelite prior to its crystallization.

Fibrolite stage (VR491, VR496)

Although there is no direct evidence for a stage where nodules were composed of fibrolite, several indications point to this occurrence. They include: (i) the presence of fibrolite in close association with the nodules

formerly occupied by garnet; (ii) the radiating arrangement of needles diverging from the nodule; (iii) the presence of biotite with exsolution of ilmenite; and (iv) the proposed crystallization sequence, in which fibrolite pre-dates kyanite. These data are suggestive of the high-T reaction of garnet to fibrolite + Ti-rich biotite, and are supported by fibrolite textures, similar to the 'disharmonious' type of Vernon & Flood (1977). Thermodynamic modelling of this reaction (Foster, 1986) predicts a complex behaviour for garnet, which may dissolve, grow or not react at all depending on the local configuration of matrix. This is in agreement with the presence, in sample VR491, of untransformed garnet crystals adjacent to partially or completely pseudomorphed ones (see Fig. 3a).

Kyanite stage (VR491, VR496)

This is represented by the nodules of microgranular kyanite, which maintain the primary shape of garnet but are not considered to replace it directly. The very fine grain size of kyanite in the nodules is an anomalous feature for metapelites; this peculiarity, and its possible cause, is discussed below.

As it is not clear whether sericite pre-dates kyanite or is coeval with it, the possibility of a further stage predating the kyanite stage, and represented by sericite crystallization (*sericite stage*), has to be considered. Sericite would form 'shimmer aggregates' replacing fibrolite, and leaving relict needles within quartz and muscovite adjacent to nodules.

Staurolite stage (VR491, VR496, VR480)

This stage, initiated in sample VR491 and completed in sample VR480, produces the nodules of microgranular staurolite. Microstructures indicate that staurolite crystallization is coeval with that of andalusite, or commenced slightly before and continued during andalusite growth. As a consequence, the staurolite stage is related to the contact metamorphism.

Muscovite stage (VR466)

This is the final stage, in which decussate aggregates of muscovite replace staurolite. Although this kind of pseudomorph is common during retrograde metamorphism, even in this area (e.g. Borsi *et al*., 1973), in this sample it has been shown to represent a prograde feature. Similar prograde pseudomorphs of muscovite after staurolite were described by Guidotti (1968) in a regional metamorphic context.

DISCUSSION

Timing of the different stages

The textural stages recognized above result from superposition of at least three metamorphic episodes starting in pre-Alpine times and terminating with the Oligocene contact metamorphism. Based on the mineral assemblages observed during the various stages, the sequence can be fitted within the evolution of the Austroalpine block north of the DAV line, tentatively reconstructed in the P–T–t path of Fig. 6, and each stage referred to a particular metamorphic event.

The garnet and fibrolite stages, the latter representing the direct replacement of garnet in these rocks, are likely to belong to a continuous, prograde metamorphism reaching amphibolite facies conditions. This situation, together with localized anatexis of pelitic lithologies, occurred on a regional scale during the Hercynian (Stöckhert, 1985). An Alpine age cannot be attributed to the first two stages, because the Alpine metamorphism never exceeded greenschist facies ($T = 450 \pm 50$ °C, Contini & Sassi, 1980; Stöckhert, 1984).

The age of the kyanite stage is controversial. Bellieni (1974) and Stöckhert (1985) interpreted the microgranular kyanite as Eo-alpine, and considered it to postdate fibrolite. However, recent microstructural re-investigation of similar rock types (Mazzoli & Moretti, 1998) suggests instead that kyanite pre-dates fibrolite, and that both polymorphs are Hercynian. The microstructural data presented in this study definitely favour the hypothesis of an Eo-Alpine age: in sample VR491 fibrolite appears only as a relict inclusion in quartz or muscovite, partially replaced by sericite, whereas kyanite occurs throughout the rock and overgrows, or is coeval with sericite.

If an independent sericite stage occurred, its age could be either Hercynian, younger than fibrolite, or

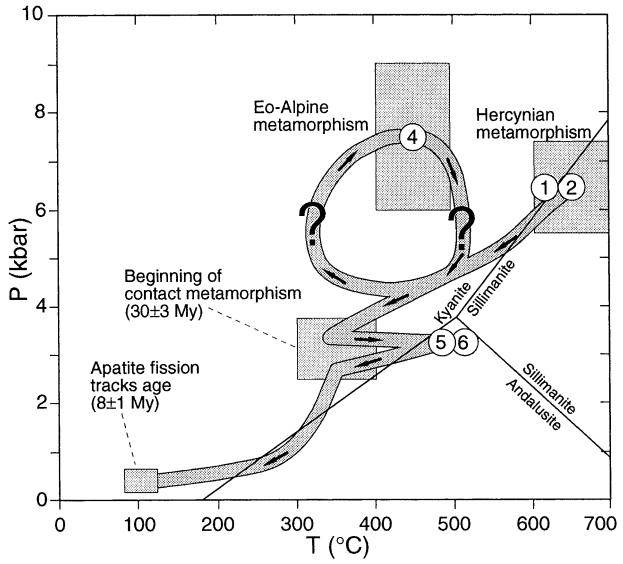

Fig. 6. Schematic P–T–t path for the Austroalpine basement north of the DAV line, with inferred location of the stages described in this study. 1, garnet stage; 2, fibrolite stage; 4, kyanite stage; 5, staurolite stage; 6, muscovite stage. Modified from Cesare & Hollister (1995) with P–T data from Stöckhert (1985, 1987). The path drawn between Hercynian and Eo-Alpine metamorphism is poorly constrained.

Eo-Alpine, older than kyanite. However, because sericitization during an hydration event could have occurred at any time between the Hercynian thermal peak and the greenschist facies Eo-alpine event, assessment of the age of sericite is not possible.

The staurolite and muscovite stages are definitely related to Oligocene metamorphism in the contact aureole of Vedrette di Ries (Cesare & Grobety, 1995). The inferred age of the stages can be summarized as in Table 2.

Age of the main foliation

According to the model proposed by Schulz (1997), the structures observed in the study area should be Hercynian in age; on the other hand, Borsi *et al.* (1978) and Mager (1985) defined the main foliation as Alpine. This foliation corresponds to the mineralogical layering observed in all samples; its age can be constrained by means of the microstructures of sample VR491. Because the nodules of kyanite and the surrounding felts of sericite do not represent competent domains that are able to partition deformation into the adjacent matrix, the anastomosing of the foliation around them must have occurred *prior* to the formation of the kyanite nodules. The most plausible interpretation is that such anastomosing was caused by the presence of rigid garnet, later pseudomorphed as described above. Thus, the development of the main foliation pre-dates the kyanite stage and the possible sericite stage, and can be syn- or post-kinematic with respect to the garnet stage. This confirms the Hercynian age of the main foliation, as proposed by Schulz (1997). This conclusion is valid only for the specific area where the samples were collected. In fact, pervasive Alpine deformation is already widespread both a few hundred metres northwards, and further south, close to the DAV line.

Common protolith and model reactions

The proposed model of a common protolith, and the possible reactions that occurred at and between each sample locality, are the subject of a companion paper that addresses these topics on the basis of chemical data. Here, only the relevant field and textural observations are highlighted.

The special microstructures here described have been observed only in the four sampled rock layers. Because the adjacent metapelites, although displaying comparable metamorphic assemblages, never contain the nodules pseudomorphing garnet, a distinctive rock type is likely to be required for the formation of these pseudomorphs. It is suggested that the four samples have such common distinctive protolith, that formed either layers within a metapelitic sequence, or one single horizon, isoclinally (re)folded and now outcropping at several localities.

Table 2. Inferred ages and metamorphic settings for the microstructural stages defined in this work.

Stage	Age	Setting
Grt	Hercynian	Regional
Fib	Hercynian	Regional
Ser	Hercynian? Eo-Alpine?	Regional
Ky	Eo-Alpine	Regional
St	Oligocene	Contact
Ms	Oligocene	Contact

Based on the appearance, disappearance and changes in abundance of minerals in nodules and matrix, model reactions can be proposed for some of the transitions between stages. Transition from the kyanite (sample VR491) to the staurolite stage (completed in sample VR480) is of the type

$$\mathrm{Ky} + \mathrm{Grt} + \mathrm{Ms} + \mathrm{Chl} = \mathrm{St} + \mathrm{And} + \mathrm{Bt} \qquad (1)$$

whereas change from the staurolite (VR480) to the muscovite stage (VR466) is of the type

$$\mathrm{St} + \mathrm{And} + \mathrm{Chl} + \mathrm{Ms} = \mathrm{Bt} + \mathrm{Sil} \qquad (2)$$

Both reactions involve two Al_2SiO_5 polymorphs: given the polymetamorphic evolution of the rocks, and the distance between samples, they should not be considered real equilibria in the AFM system. In fact, they are very likely to represent the sum of an Al_2SiO_5 polymorphic transition with a (disequilibrium?) reaction involving the ferromagnesian phases.

Significance of microgranular kyanite

The common occurrence of kyanite and staurolite as porphyroblasts in metapelites is in contrast with the fine grain size (100–200 μm) in which they occur in the nodules. In the case of staurolite, the microgranular texture of samples VR496 and VR480 can be explained by epitaxial replacement of kyanite. Thus, a new crystal of staurolite grows for each kyanite grain, and the resulting grain size is comparable to that of precursor kyanite, except for staurolite crystals at the rim of nodules, which can freely overgrow the adjacent sericite. It is then apparent that this microstructure can only form where a former aggregate of microgranular kyanite is present.

Interpretation of the microgranular kyanite is more problematic. This peculiar texture, first documented in the area by Bellieni (1974), has been reported from other parts of the Eastern Alps (e.g. Kleinschmidt, 1970) and the Western Alps (e.g. Dal Piaz, 1971). It is also reported from Scotland (Tilley, 1935) and the Spanish Betic Cordillera (Puga *et al.*, 1975). All the described rocks are polymetamorphic, with a low-T, medium- to high-P metamorphism overprinting high-grade metamorphism. Microgranular kyanite is related to the low-T/high-P event, and has been interpreted as a static pseudomorph after sillimanite (Dal Piaz, 1971) or andalusite (e.g. Puga *et al.*, 1975). Because this particular metamorphic context is also very similar to that of sample VR491, it must be critical for the

formation of microgranular kyanite, and the plausible genetic model is likely to be applicable to all these occurrences.

This microstructure can be interpreted taking into account the kinetic controls on texture development. The main differences with usual formulations modelling the case of prograde metamorphism (e.g. Kerrick *et al*., 1991) are that in the present example the degree of overstepping of reaction boundary is large and negative. Formation of microgranular aggregates requires very high nucleation rates and low growth rates; both are a positive function of the degree of overstepping of a reaction boundary, but nucleation rate increases much more rapidly (Ridley & Thompson, 1986). Growth rates, either diffusion-controlled or reaction-controlled, are also proportional to the absolute temperature at which reaction occurs. In addition, the kinetic role of deformation is also critical to the process, as deformation both enhances mass transfer between reaction sites and lowers the degree of overstepping required for nucleation.

Because in sample VR491 fibrolite replacement by kyanite occurs under:

(i) 200 ± 50 °C overstepping of the sillimanite = kyanite reaction boundary,
(ii) relatively low absolute temperature (450 ± 50 °C),
(iii) static conditions,

very high nucleation rates and low growth rates are to be expected, producing the microgranular texture.

I conclude that mono-mineralic aggregates of microgranular kyanite should form as pseudomorphs after a precursor Al_2SiO_5 polymorph, whenever high-grade metapelites are involved in subsequent, static, low-T/high-P metamorphism.

ACKNOWLEDGEMENTS

Financial support from MURST and CNR. I thank L. Hollister for discussion in the field, C. Brogiato and S. Castelli for help with photomicrographs, F. P. Sassi, B. Schulz, R. Spiess and R. Vernon for comments on earlier versions of the manuscript, and M. Ballèvre, M. Guiraud and D. Robinson for their reviews. This work would have been much more difficult without the help of G. Leitgeb at the Rieserferner Hütte.

REFERENCES

Bellieni, G., 1974. Sugli aggregati microgranulari di cianite esistenti nei micascisti austridici a nord-ovest di Brunico (Alto Adige). *Studi Trentini di Scienze Naturali*, **51,** 105–112.

Borsi, S., Del Moro, A., Sassi, F. & Zirpoli, G., 1973. Metamorphic evolution of the Austridic rocks to the south of the Tauern window (Eastern Alps). Radiometric and geopetrologic data. *Memorie della Società Geologica Italiana*, **12,** 549–571.

Borsi, S., Del Moro, A., Sassi, F. P., Zanferrari, A. & Zirpoli, G., 1978. New petrologic and radiometric data on the Alpine history of the Austridic continental margin south of the Tauern window (eastern Alps). *Memorie di Scienze Geologiche*, 32, 1–17.

Brodie, K. H. & Rutter, E. H., 1985. On the relationship between deformation and metamorphism with special reference to the behaviour of basic rocks. In: *Metamorphic Reactions. Kinetics, Textures and Deformations* (eds Thompson, A. B. & Rubie, D. C.). *Advances in Physical Geochemistry*, **4,** 138–179.

Carmichael, D. M., 1969. On the mechanism of prograde metamorphic reactions in quartz-bearing pelitic rocks. *Contributions to Mineralogy and Petrology*, **20,** 244–267.

Cesare, B., 1994. Hercynite as the product of staurolite decomposition in the contact aureole of Vedrette di Ries, eastern Alps, Italy. *Contributions to Mineralogy and Petrology*, **116,** 239–246.

Cesare, B. & Grobety, B., 1995. Epitaxial replacement of kyanite by staurolite: a TEM study of the microstructures. *American Mineralogist*, **95,** 78–86.

Cesare, B. & Hollister, L. S., 1995. Andalusite-bearing veins at Vedrette di Ries (Eastern Alps – Italy): fluid phase composition based on fluid inclusions. *Journal of Metamorphic Geology*, **13,** 687–700.

Contini, R. & Sassi, F. P., 1980. Su alcuni effetti metamorfici Alpini nel basamento austridico in Pusteria. *Memorie di Scienze Geologiche*, **34,** 187–194.

Dal Piaz, G. V., 1971. Nuovi ritrovamenti di cianite Alpina nel cristallino antico del Monte Rosa. *Rendiconti Società Italiana di Mineralogia e Petrologia*, **27,** 437–477.

Foster, C. T., 1986. Thermodynamic models of reactions involving garnet in a sillimanite/staurolite schist. *Mineralogical Magazine*, **50,** 427–439.

Fyfe, W. S., Price, N. J. & Thompson, A. B., 1978. *Fluids in the Earth's Crust*. Elsevier, Amsterdam.

Guidotti, C. V., 1968. Prograde muscovite pseudomorphs after staurolite in the Rangeley-Oquossoc areas, Maine. *American Mineralogist*, **53,** 1368–1376.

Kerrick, D. M., Lasaga, A. C. & Raeburn, S. P., 1991. Kinetics of heterogeneous reactions. In: *Contact Metamorphism* (ed. Kerrick, D. M.). *Reviews in Mineralogy*, **26,** 43–104.

Kleinschmidt, G., 1970. Metamorphose und Stratigraphie im Kristallin der südlichen Saualpe (Ostalpen) *Abhandlungen des Naturwissenschaftlichen Vereins in Hamburg*, **14,** 81–144.

Kleinschrodt, R., 1987. Quarzkorngefugeanalyse im Altkristallin südlich des westlichen Tauernfensters (Sudtirol/Italien). *Erlanger Geologische Abhandlungen*, **114,** 1–82.

Mager, D., 1985. Geologische Karte der Rieserfernergruppe zwischen Magerstein und Windschar (Sudtirol). *Der Schlern*, **6,** 1–26.

Mazzoli, C. & Moretti, A., 1998. Alpine alteration of kyanite aggregates from Cima Valperna area (Austroalpine basement, Eastern Alps). *Plinius*, **20,** 151–152.

Puga, E., Fontboté, J. M. & Martìn-Vivaldi, J. L., 1975. Kyanite pseudomorphs after andalusite in polymetamorphic rocks of Sierra Nevada (Betic Cordillera, Southern Spain). *Schweizerische Mineralogische und Petrographische Mitteilungen*, **55,** 227–241.

Ridley, J., 1985. The effect of reaction enthalpy on the progress of a metamorphic reaction. In: *Metamorphic Reactions. Kinetics, Textures and Deformations* (eds Thompson, A. B. & Rubie, D. C.). *Advances in Physical Geochemistry*, **4,** 80–97.

Ridley, J. & Thompson, A. B., 1986. The role of mineral kinetics in the development of metamorphic microtextures. In: *Fluid–Rock Interactions During Metamorphism* (eds Walther, J.V. & Wood, B. J.). *Advances in Physical Geochemistry*, **5,** 154–193.

Sassi, F. P., Zanettin, B. & Zirpoli, G., 1980. Quadro della storia termica Alpina nelle Alpi Orientali. *Rendiconti Società Italiana di Mineralogia e Petrologia*, **36**, 19–33.

Sassi, F. P., Zanferrari, G. & Zirpoli, G., 1987. The Caledonian event in the Eastern Alps: a review. In: *Pre-Variscan and Variscan Events in the Alpine-Mediterranean Mountain Belts* (eds Flügel, H. W., Sassi, F. P. & Grecula, P.), pp. 431–434. Alfe Publisher, Bretislava.

Schulz, B., 1995. Rekonstruktion von P–T–t–d-Pfaden der Metamorphose: Mikrostrukturell kontrollierte Geothermobarometrie in Metapeliten und Metabasiten der variskischen Internzone (Ostalpen, Nordost-Bayern, Aiguilles

Rouges Massif, Massif Central). *Erlanger Geologische Abhandlungen*, **126,** 1–222.

Schulz, B., 1997. Pre-Alpine tectonometamorphic evolution in the Austroalpine basement to the south of the central Tauern Window. *Schweizerische Mineralogische Petrographische Mitteilungen*, **77,** 281–297.

Selverstone, J., 1985. Petrologic constraints on imbrication, metamorphism and uplift in the SW Tauern Window, Eastern Alps. *Tectonics*, **4,** 687–704.

Stöckhert, B., 1984. K–Ar determinations on muscovites and phengites from deformed pegmatites, and the minimum age of the Old Alpine deformation in the Austridic basement to the south of the western Tauern window (Ahrn valley, Southern Tyrol, Eastern Alps), *Neues Jahrbuch für Mineralogie, Abhandlungen*, **150,** 103–120.

Stöckhert, B., 1985. Pre-Alpine history of the Austridic basement to the south of the Tauern Window (Southern Tyrol, Italy) – Caledonian versus Hercynian event. *Neues Jahrbuch für Geologie Paläontologie, Monatshefte*, **10,** 618–642.

Stöckhert, B., 1987. Das Uttenheimer Pegmatit-Feld (Ostalpines Altkristallin, Südtirol) Genese und alpine Überprägung. *Erlanger Geologische Abhandlungen*, **114,** 83–106.

Tilley, C. E., 1935. The role of kyanite in the 'hornfels zone' of the Carn Chuinneag granite (Ross-shire). *Mineralogical Magazine*, **149,** 92–97.

Vernon, R. H. & Flood, R. H., 1977. Interpretation of metamorphic assemblages containing fibrolitic sillimanite. *Contributions to Mineralogy and Petrology*, **59,** 227–235.

Wheeler, J., Treloar, P. J. & Potts, G. J., 1995. Structural and metamorphic evolution of the Nanga Parbat syntaxis, Pakistan Himalayas, on the Indus gorge transect: the importance of early events. *Geological Journal*, **30,** 349–371.

Yardley, B. W. D., 1977. The nature and significance of the mechanism of sillimanite growth in the Connemara Schists, Ireland. *Contributions to Mineralogy and Petrology*, **65,** 53–58.

Received 26 November 1997; revision accepted 7 June 1999.